JOURNAL OF AIRCRAFT
Vol. 48, No. 4, July–August 2011

Refined Numerical Simulation of Three-Dimensional Riveting in Laminated Composites

Tae Ho Yoon* and Seung Jo Kim†
Seoul National University, Seoul 151-744, Republic of Korea

DOI: 10.2514/1.C031311

Riveting in laminated composites is not carried out, because the riveting process can easily induce failure and form a nonuniform interference fit. An electromagnetic riveting riveter provides a relatively uniform interference fit with no direct failure in the riveted joint. Finite element numerical simulation of three-dimensional riveting is conducted by considering the sine wave of force history for the electromagnetic riveting riveter. To reflect the physical phenomenon of the complicated contact of riveting in laminated composites, a refined modeling of the washer inner fillet is considered, and the parallel computations using LS-DYNA are used. Refined simulation is validated by experiments reported in the literature. The electromagnetic riveting is properly applied for riveting in laminated composites. Optimized maximum riveting force is obtained for relative uniform interference based on the criterion of relative interference for fatigue life extension. A parametric study of the washer effects during the riveting process is investigated to obtain a proper riveted joint in laminated composites.

Nomenclature

A	=	yield stress
B	=	parameter by strain hardening law
c	=	stain-rate parameter
D	=	diameter of driven rivet head
d	=	initial diameter of aperture
D_0	=	diameter of initial rivet shaft
D_1	=	diameter of deformed rivet shaft
F	=	riveting force
$F_{\max}$	=	maximum force
h	=	installed rivet-tail height
h_0	=	uninstalled rivet-tail height
n	=	parameter by strain hardening law
R	=	radius of initial rivet shaft
r	=	distance of lateral direction from rivet shaft axis
t	=	current time
t_0	=	riveting time
ε	=	effective plastic strain
$\dot{\varepsilon}$	=	strain rate
σ_y	=	flow stress

I. Introduction

A MECHANICAL joint is mainly used to connect structures constructed by using the same or different materials because it is useful in large force transfers and easy to repair. A riveted joint is a type of mechanical joint, like a pinned joint and a bolted joint, used to reduce the production time and cost of structures, such as an aircraft that has many connected parts. Laminated composites are used more and more in aircraft due to their high strength/weight and stiffness/weight ratios, compared with metallic materials. Riveting usually does not work properly in laminated composites, although a riveted joint in laminated composites has an important role in aircraft structures, which need to be lightweight. Three types of aircraft sheet structures for riveting may be classified as follows: metal–metal [1,2], metal–composite [3], and composite–composite [4]. Another type of material may be fiber–metal laminate (FML) [5].

Riveting is an important procedure for applying an interference fit. It induces compressive residual stress, which enhances the fatigue life of a riveted joint [2,6]. The parameters that affect the riveting process are the rivet type, the rivet head angle, the material of the rivet and sheets, clearance, and the engineer's skill in avoiding misalignment between the sheets and the rivet, which has an important effect on the fatigue life of a riveted joint. Riveting in laminated composite structures has not been used until recently because of its $60 \sim 85\%$ failure rate at the joint of a composite structure compared with that of a metallic structure [4]. There are two kinds of riveters: one is the conventional riveter, such as the pneumatic riveter or the hydraulic riveter, and the other is the new type, the electromagnetic riveter (EMR). Composite structures have low interlaminar strength, so riveting using a conventional riveter (hydraulic or pneumatic riveter) in composite structures may lead to abrupt rivet deformation and, as a result, cause direct failure at the start of the riveting process. Furthermore, the nonuniform interference fit in the riveted joint may shorten fatigue life. Therefore, pins or bolts have been used mainly to join composite structures.

Fatigue life can be increased by the compressive residual stress generated from the application of an interference fit to a hole located essentially in the joint part of metallic and composite structures [7,8]. Interference strengthening technologies have been commonly used to enhance the fatigue life of metal assemblies and to expand the service life of metal structures [8,9]. Torque transmission is applied by tightening the shafts and wheels in which the interference fit is usually used. In the case of a riveted joint, the conventional riveting method is commonly used to make the interference fit between the rivet and the aperture wall. However, a rivet joint in laminated composites by conventional riveting techniques has more difficulty in controlling the interference fit than a bolted joint. Although a riveted joint installed in metallic structures by a conventional riveter may still be exposed to crack problems, it is often used in many applications because there is no limitation on the use of an interference fit, unlike the case in composite structures [1,10].

A uniform interference fit improves the fatigue life of a riveted joint [4], so a riveter that can make a uniform interference fit is needed. In the case of riveting in laminated composites, there must be no initial failure by an impact force from an impact distance at the start of riveting. The riveting force of the EMR riveter is a kind of impact force applied at an impacting distance of zero. Zero impacting distance induces very little impacting damage to a structure in EMR riveting, unlike pneumatic or hydraulic riveting [4]. An EMR riveter also has a high-speed riveting time, which is advantageous in making a uniform interference fit. EMR (named as the stress-wave rivet

Received 14 November 2010; revision received 30 March 2011; accepted for publication 30 March 2011.

*Ph.D. Candidate, School of Mechanical and Aerospace Engineering, 1 Gwanak-ro, Gwanak-gu; auseyoon@aeroguy.snu.ac.kr.

†Professor, School of Mechanical and Aerospace Engineering, 1 Gwanak-ro, Gwanak-gu; sjkim@snu.ac.kr. Fellow AIAA.

system in [11]) could be used for composite structures. Experimental riveting in fiber composite with an EMR riveter showed no direct failure and formed a uniform interference fit [4]. These experimental tests were carried out based on the criterion that interference should be less than 2% relative interference to extend fatigue life and to prevent damage to the aperture wall [12]. The rivet formation dynamics of an EMR riveter is different from those of pneumatic and hydraulic riveters. The conventional riveters take ∼0.5 s, while an EMR riveter takes $1 \sim 2$ ms to make a riveted joint [13]. An EMR riveter can make a uniform interference fit along the rivet shaft, as it simultaneously expands the rivet shaft because of its high speed [4]. Although a conventional riveter is mainly used for joints, an EMR riveter is used more often in the aircraft industry, as well as the car industry, because of its lightness [4,14,15]. An EMR riveter can be used for riveting in composite structures without causing any failure [3,4].

Recently, interference fit riveting in metallic-composite structures using an EMR riveter was investigated numerically and experimentally [3]. The compressive residual stress and rivet formation beneath the rivet head that are generated during the riveting process were investigated effectively by finite element (FE) numerical simulation. However, experimental measurement methods, such as neutron diffraction [16] or pressure-sensitive film [10], can be used just after the riveting process. Until now, numerical analysis of riveted joints usually dealt with compressive residual stress considering the ideal interference fit instead of an actual interference fit obtained from the riveting process [17], and the results of these analyses were applied to the design of a riveted joint. On the other hand, numerical analysis of a riveted joint was conducted by using the initial compressive residual stress obtained from riveting simulation [10,18]. Although a fine three-dimensional (3-D) riveting modeling has become possible with advancements in computation capacity, two-dimensional (2-D) modeling is still used to obtain simplified results and to save computational costs [3]. Three-dimensional modeling allows us to understand the effects of various parameters, such as residual stress, rivet deformation, and misalignment of the rivet beneath the rivet head [1,5,10,19]. Parallel computing can be used for the simulation of detailed modeling, with many degrees of freedom to quickly change a design of a product for rapid manufacturing at low cost [20]. Specifically, riveting simulation with fine 3-D modeling using parallel computing can be used to analyze the physical phenomenon of complicated contacts in more detail, rapidly, and at low cost. Holleman and Muller [5] studied the riveting in a FML material bonded from glare and aluminum, instead of a metallic material, according to the decrease of the weight of the joint structure. The EMR riveting in a metal composite was investigated by Deng et al. [3], numerically and experimentally. In the numerical study [3], the riveting modeling, which was a 2-D coarse mesh, predicted no interference fit effects. However, a numerical study of riveting in a composite–composite structure has been carried out in a few works [21,22], even after an experiment in the literature [4] reported successful riveting in fiber-laminated composites. Three-dimensional riveting simulations according various parameters, clearances, and washer dimensions, which were compared with experimental results, did not consider fine modeling and EMR riveter characteristics [21].

Direct riveting in laminated composites is challenging, so there has been limited research related to experiments or numerical analysis of EMR riveting in laminated composites. EMR riveting in laminated composites is a new field in riveting techniques, and related works will appear gradually.

II. Electromagnetic Riveting Mechanism

EMR is a new type of riveting technique based on eddy current repulsion between copper pancake coils. At first, electromagnetic forming equipment was used in metal forging and forming due to its large size, but it was difficult to apply in riveting. Later on, it was applied to riveting in composite structures by using a stress-wave rivet system. Light EMR riveters have been used frequently in the aircraft or car industry. The EMR riveter is composed of a rivet die, a driver, a body damper, a spring, etc., as shown in Fig. 1. EMR motion is controlled by two actuators, typically on opposing sides of the rivet. Each actuator is connected to its own capacitor bank by a coaxial pulse cable. After the capacitors have been charged to a predetermined voltage, this stored energy is discharged through the coil. An intense magnetic pressure quickly develops between the coil and the driver plate, accelerating the driver into the rivet [4]. The detailed information of the EMR technique is provided in the literature [4,14].

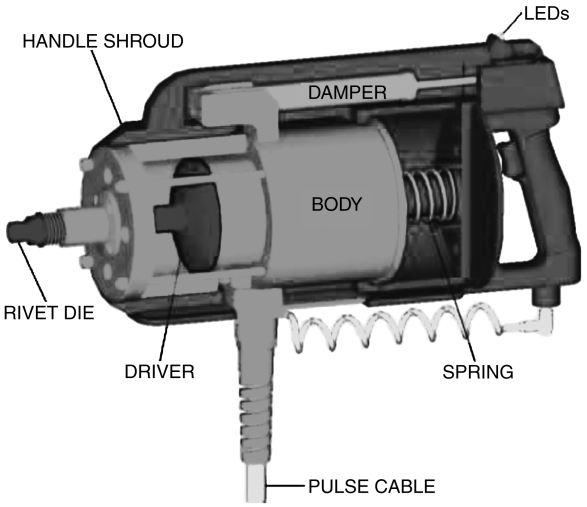

Fig. 1 HH503 actuator cutaway [14] (LED denotes light-emitting diode).

The riveting force of the EMR riveter is a kind of impact force applied at an impacting distance of zero, which induces very little impacting damage to a structure compared with the riveting force of the pneumatic or hydraulic riveter [4]. The magnetic force history induced from the EMR is directly transferred to the riveting force history. The first wave is used as the main riveting force followed by some decreasing waves of the first wave, which do not contribute to the riveting force [23]. This riveting force forms a large plastic deformation, which induces a high strain rate during the riveting process.

Electromagnetic technology is an important research field in forging, forming, and riveting. Therefore, an electromagnetism (EM) module is installed in commercial software such as ANSYS and LS-DYNA. EM modules of shared memory parallel and massively parallel processing (MPP) versions in LS-DYNA/V971 have been developed recently [24]. Deng et al. [3] used the electricity and magnetism coupled analysis of ANSYS/multiphysics to obtain the magnetic force history. An EMR riveter is a force-controlled riveter, which provides greater consistency in the compressive residual stress field produced than the conventional riveters throughout the rivet installation process. In a riveting simulation, a sine wave force history is considered, because the exact force to be applied on a die is unknown [25]. In other cases, a linear force history is considered [2].

III. Riveting Modeling

A. Geometry

FE modeling is carried out for a directly riveted overlapped region to investigate the effect of an interference fit on the geometry of a single riveted lap joint. Overall model features and dimensions for the riveting simulation are shown in Fig. 2. The model for the refined 3-D riveting is referenced from the base model [21].

The FE riveting model is composed of a rivet, a washer, and upper and lower sheets of the laminated composite, as shown in Fig. 2. The rivet is a countersunk rivet with a shaft diameter of 4.0 mm, a countersunk diameter of 8.72 mm, and a depth from the rivet head (height) of 2.00 mm. The rivet's countersunk angle is 100 deg. The upper and lower sheets are made of laminated composites. The thickness of each lamina is 0.13 mm. There are a total of 24 layers,

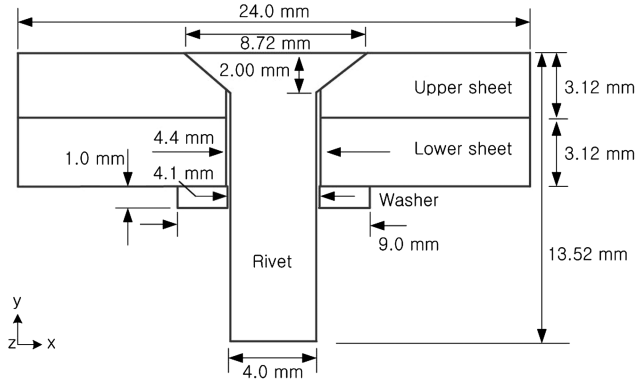

Fig. 2 2-D schematic of 3-D model.

and there are no intervals between the layers. The laminated composite has a quasi-isotropic layup $[+45/-45/0/90]_{3s}$ and, for the model, it is rectangular of dimensions (24.0×24.0 mm).

The interference fit in composite structures by riveting is controlled by two methods. One method increases the clearance between the rivet shaft and aperture wall, and the other restricts the shaft expansion using a washer [4]. If the clearance is too wide, a deformed shaft may be misaligned and, as a result, the joint strength may be decreased. A special washer can prevent an excessive interference fit in the area of the rivet tail. Interference fit control using a washer is more effective than increasing the clearance [4]. The washer's outer diameter is 9.0 mm, the inner diameter is 4.1 mm, and the thickness is 1.0 mm. A special washer is needed to rivet laminated composite structures different from the washer used for metallic structures. The inner diameter of the washer controls the expansion of the rivet, the outer diameter decides the force-carrying area during rivet formation, and the thickness decides the stiffness of the washer [4].

The relative interference is measured by the following formula in Eq. (1) [4]:

$$\text{relative interference} = \frac{D_1 - d}{d}(\%) \tag{1}$$

where D_1 is the diameter of the deformed shaft, and d is the initial diameter of the aperture.

B. Material of Model

The materials of the rivet, washer, and laminated composite material are given in Table 1.

Titanium is used for the rivet and washer because it effectively resists galvanic corrosion [10]. The simplified Johnson and Cook (J–C) model, as described by Eq. (2), is selected to consider the large deformation and high strain rate produced by the high-speed riveter. This material is material type 98 (MAT_SIMPLIFIED_JOHNSON_COOK) in LS-DYNA [26]. This form is chosen for its relative simplicity and the absence of a clearly better simple model [27]. The model of this material is simpler than the J–C model because it neglects the temperature effects in the flow stress:

$$\sigma_y = (A + B\varepsilon^n)(1 + c\,\ell_n\,\dot{\varepsilon}) \tag{2}$$

where σ_y is the flow stress (applied force per unit area), A is the yield stress (transition from elastic to plastic regime), B and n are the parameters in the strain hardening law, c is the stain-rate parameter, ε is the effective plastic strain, and $\dot{\varepsilon}$ is the strain rate. The rivet (titanium) is modeled with $A = 200$ MPa, $B = 700$ Mpa, $n = 0.22$, and $c = 0.06$ [28].

The washer material used in [28] is type 3 (MAT_PLASTIC_KINEMATIC) in LS-DYNA. The washer has a yield stress of 500 MPa and a linear hardening modulus of 200 MPa. The composite part is made from material manufactured from the carbon epoxy prepreg material with nominal fiber volume fraction 63.5%. Material type 2 (MAT_ORTHOTROPIC_ELASTIC) in LS-DYNA is selected for the composite structure; failure effects are not considered, and elastic behavior is considered. Riveting in laminated composites is analyzed, considering the fatigue life expansion of a composite material for relative interference within 2% [4,12].

C. Force and Boundary Condition

The force condition is like that of an EMR riveter on a rivet tail moving directly toward the rivet shaft direction. The riveter is moved by a sine wave riveting force history. As the force decreases, a springback effect occurs in the rivet. The riveting force is transferred to the rivet tail, as shown in Eq. (3):

$$F(t) = \begin{cases} F_{\max} \sin \frac{\pi t}{t_0} & t \le t_0 \\ 0 & t > t_0 \end{cases} \tag{3}$$

where $F_{\max}$ is the maximum force of the EMR riveter, and t_0 is the riveting time.

For the boundary condition, the rivet centerline along the rivet shaft is allowed to move in the y direction ($x = z = 0$) to prevent rivet misalignment. The rivet shaft direction is also constrained on the rivet head ($y = 0$). There is no constraint in the laminated composites because the rivet and washer constrain the movement of the laminated composites.

Contact definition is specified using the segment-based automatic contact options (CONTACT_AUTOMATIC_SURFACE_TO_SURFACE) in LS-DYNA. Surface interaction is defined as contact pairs using the master–slave algorithm available in LS-DYNA. A coefficient of friction of 0.3 is applied for the rivet–sheet, sheet–sheet, and sheet–washer contacts. A FE study is conducted as a dynamic explicit process. Any thermal process is ignored in the simplified J–C model.

D. Riveting Modeling

Full modeling is conducted instead of the half- or quarter-modeling with consideration of symmetric conditions, which are usually applied in papers [1,2,18] to save computation time and cost. Refined modeling of the rivet, washer, and laminated composites based on the mesh sensitivity test [22] that used base modeling [21] is constructed as shown in Fig. 3a. Each part of the full modeling is shown in Fig. 3b.

The total numbers of nodes and elements are 210,500 and 195,872, respectively, in the whole riveting modeling. In the washer modeling, 0.3 mm radius fillets of the inner hole are considered to reflect the geometry of the washer and the physical characteristic of the complicated contact of riveting in laminated composites, because a washer with no fillet gives an incorrect estimation of the interference fit near the driven rivet head in rapid riveting [22]. Mesolevel modeling [29], where a laminated composite composed of 24 layers is distinguished by each layer, is conducted instead of homogenized modeling to investigate the stress in the thickness direction.

An eight-node brick element with one-point integration is used for the rivet, washer, and laminated composites. When using one-point integration, a zero energy mode, otherwise known as the hourglass mode, is usually shown. Full integration can provide not only more

Table 1 Elastic properties of materials and their constituents

Material	E_{11}, GPa	E_{22}, GPa	E_{33}, GPa	G_{12}, GPa	G_{13}, GPa	G_{23}, GPa	ν_{12}	ν_{13}	ν_{32}
Lamina [25]	140	10	10	5.2	5.2	3.9	0.3	0.3	0.5
Titanium [25] (washer)	110						0.29		
Titanium [28] (rivet)	115	——	——	——	——	——	0.35		

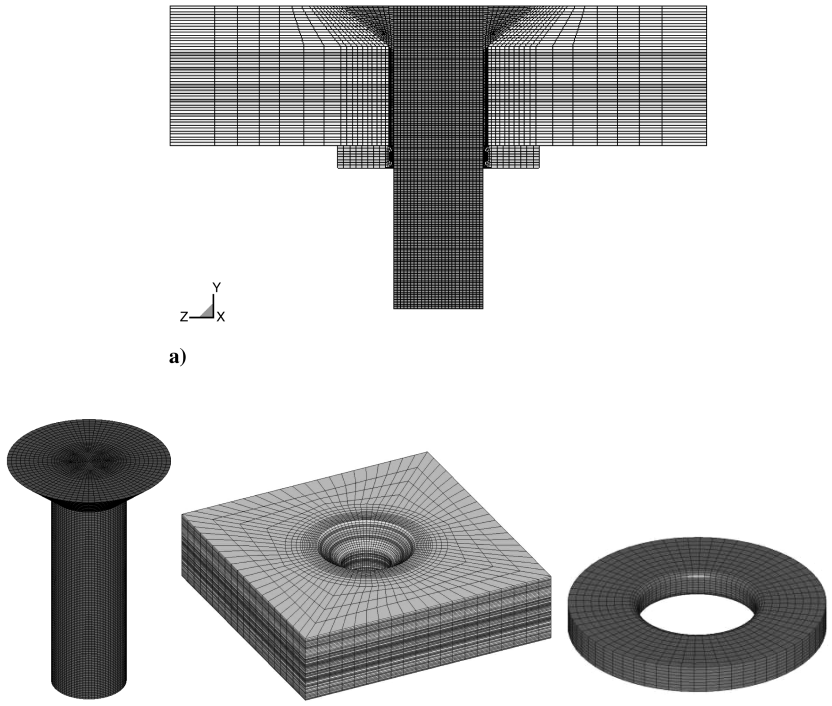

Fig. 3 Full 3-D riveting modeling : a) cross section and b) each part.

exact results than one-point integration but also avoid this hourglass mode problem. With parallel computing, riveting modeling with full integration is effective, but the technique has a locking problem and is time consuming. It is also less desirable for coarse-mesh full integration in large-deformation problems due to its element distortion sensitivity [2]. To avoid the zero energy mode, the stiffness control mode with exact volume of type 5 (Flanagan–Belytschko stiffness form with exact volume integration) in LS-DYNA is applied. In the case of the viscous hourglass control mode (hourglass control types 1, 2, and 3 in LS-DYNA), some elements of countersunk parts are distorted, and parameters may needed to be controlled. A four-node plate element is used to model the EMR riveter as a rigid body. Neither time scaling nor mass scaling is used to save computing time, because parallel computing is used for the simulation of refined 3-D modeling. A numerical technique, such as dynamic relaxation or remeshing, which is a method applied in riveting because of large deformation of the rivet tail, is not considered because it uses full modeling and a relatively small mesh size in the refined modeling.

For geometric construction and modeling, MSC/Patran and FEMB/V28 are used. LS-DYNA [26], a nonlinear transient explicit FE analysis program from Livermore Software Technology Corporation, is used for the riveting simulation. Two parallel versions of MPP in LS-DYNA are used to analyze the refined modeling. One is tested by LS-DYNA/V970 using the Pegasus system in our laboratory, and the other is tested by LS-DYNA/V971 using the IBM machine at the Korea Institute of Science and Technology Information (KISTI). To confirm the results of the analysis, LS-PREPOST is used for postprocessing.

IV. Riveting Simulation

The riveting simulation considered the kinetic energy of the rivet head and rivet tail applied by an EMR riveter. The rivet head was constrained, and a riveting force was applied on the rivet tail. A sine wave force history and 1 ms EMR riveting time were considered in the simulation. A two-step force followed by the movement of the riveter was considered in the simulation. For rapid riveting time of 1.0 ms, the explicit FE code LS-DYNA was used.

A. Riveting Force

The riveting simulation was divided by two steps of the loading history. The first step was the loading step, in which the riveter was moved along the rivet shaft direction on a rivet tail. The next step was the unloading step, in which the riveter was removed from the rivet after the maximum force was reached. The loading step occurred from 0.0 to 0.5 ms, and the unloading step occurred from 0.5 to 1.0 ms, as shown in Fig. 4b. The EMR riveter was simulated with 35,000 N of maximum force of the sine wave force history for a riveting time of 1 ms. The riveting force was applied, as shown in Fig. 4a, and the springback effect appeared in the rivet during the unloading step, as shown in Fig. 4b. The riveter movement by the sine wave force history was the same as the rivet displacement that was shown by the riveting simulation, which means that the riveter was in contact with the rivet tail throughout the riveting process. The relation between riveting force and rivet displacement is shown in Fig. 5.

B. Verification of Riveting Model

Figure 6 shows the deformed shape of the countersunk rivet, the dimension of the driven rivet head, and the measurement location. The rivet undergoes a large elastoplastic deformation in response to an applied riveting force. In Fig. 6, location A is the lowest position of the lower sheet of the laminated composites, location B is the starting point of the faying surface between the upper and lower sheets of the laminated composites, and location C is the joint position between the countersink in the rivet head and the rivet shaft [4]. The measurement locations for the interference fit from locations C to A are set as nondimensional normalized numbers from 0.0 to 1.0.

Table 2 shows the mesh sensitivity test of washer modeling, as shown in [22]. The washer with an inner fillet of radius 0.3 mm was modeled in detail, and the simulation results for point A and point B in Fig. 6 were similar to those in the experiment literature [4]. This simulation reflected the physical phenomena of the complicated contacts of riveting in a laminated composite. The other three mesh models without the washer inner fillet gave relative interference results different from the experiment results and, in particular, the relative interference of point C of the mesh modelings was different from the results in the experiment literature. We found that the

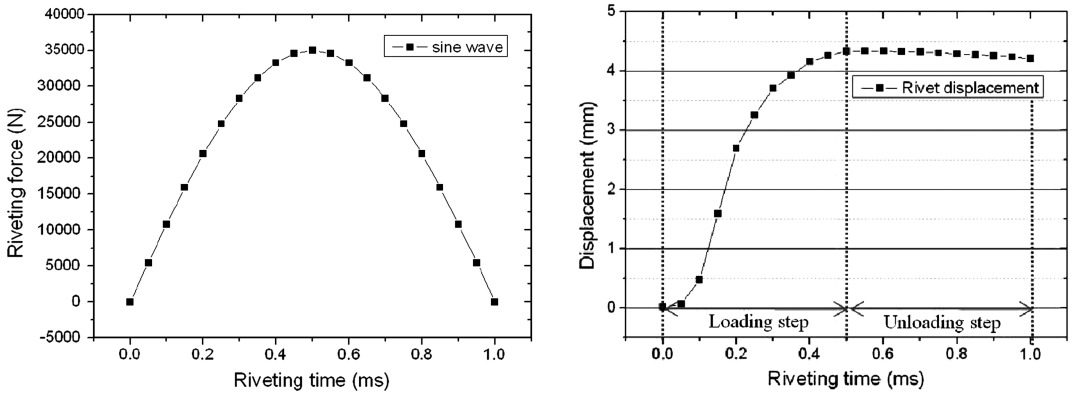

a) Riveting force **b) Rivet displacement**

Fig. 4 Riveting force and rivet displacement with time.

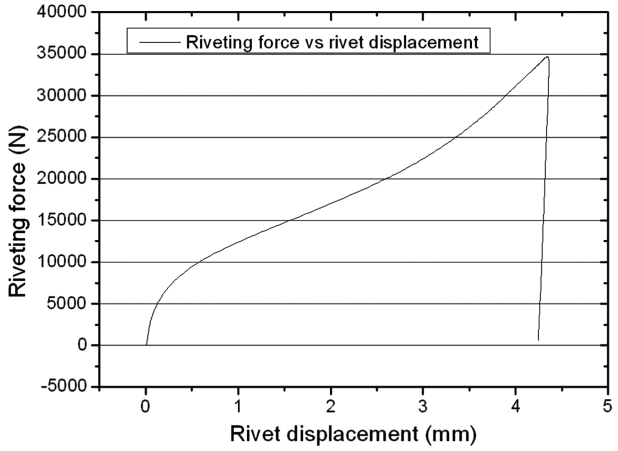

Fig. 5 Riveting force and rivet displacement.

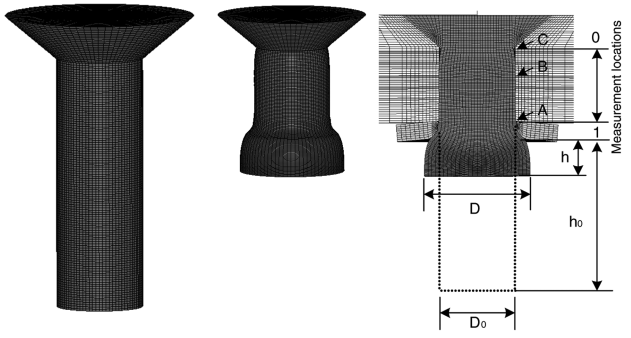

Fig. 6 Deformed shape of rivet.

interference fit along the rivet shaft of the riveting simulation depended on the mesh size of the washer model. Therefore, detailed modeling should incorporate the washer inner fillet in the simulation of riveting in laminated composites to reflect the complicated contacts among the rivet, washer, and laminated composites.

As shown in Fig. 7, the optimum maximum force for the verification of the riveting modeling is found from the trial and error method at the end of the riveting load based on the results of experiments in the literature [4]. The maximum force of 35,000 N was obtained from a few numerical simulations. Therefore, to verify the riveting modeling, 35,000 N of maximum force of sine wave force history and 1 ms of riveting time were applied to the EMR riveter. Relative interference was measured at each mesh node point of the rivet shank and was verified by experiment. The reasonable result of the interference fit was obtained except at location 0.0 (point C in Fig. 6), as shown in Fig. 7. During and after the riveting simulation, a minus relative interference, which is usually a void between the rivet shaft and the aperture wall, appeared around the normalized location 0.0. The experiment introduced about 1% relative interference at location 0.0, but exact information like the cut view of the riveted joint was not observed. The numerical simulation may need to consider a more detailed control of the material parameters of the rivet to obtain an interference fit value similar to that of the experiment at location 1.0 (point C).

The interference fit along the rivet shaft at the end of the loading step was larger than that at the end of the unloading step because of the springback effects in the rivet. As shown in Fig. 7, the relative interference at the end of the unloading step at location 0.3 (point B) and location 1.0 (point A) was in good agreement with the experimental result but not at location 0.0 (point C). Therefore, the riveting simulation of the EMR riveter was considered to have been conducted properly, except at location 0.0. From the results of the experiment literature, a nonuniform and excessive interference fit appears for a pneumatic riveter. Relative uniform interference is shown to be about 1.4% from locations of about 0.3 to 1.0. So, the riveting simulation of the EMR riveter under the condition of 1 ms riveting time and sine wave riveting force history with maximum riveting force of 35,000 N was validated with the experiments in the literature [4].

Table 2 Mesh sensitivity test of washer modeling

Mesh size of washer thickness	Washer fillet[a]	Number of washer elements	Relative interference, %		
			A point	B point	C point
1/3 mm	×	540	0.4	0.7	−5.9
1/6 mm	×	2688	0.5	0.8	−6.0
1/8 mm	×	4096	0.7	0.8	−5.9
1/8 mm	○	7168	1.6	1.2	−5.7
Experiment [4]	n/a	——	1.7	1.2	1.0

[a]×: no; ○: yes.

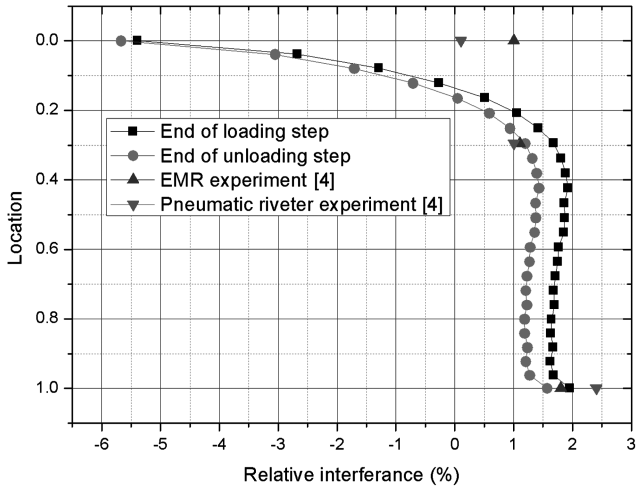

Fig. 7 Relative interference along rivet shaft at end of unloading step.

V. Results and Discussion

A. Rivet Deformation

The cut view at each time step during riveting is shown in Fig. 8. As shown in Fig. 8, effective plastic stain occurs mostly near the rivet tail, where there is a large deformation of the rivet. Figures 8a and 8b show the plastic strain during the loading step, and Figs. 8c and 8d show the plastic strain during the unloading step. Figures 8b–8d are similar but show relatively large differences of the interference fit, which greatly affected the fatigue life of the riveted joint in the laminated composites. In Fig. 8d, there is a gap between the upper sheet and lower sheet of the laminated composites due to squeezing force effects. If one or two sides of the laminated composites are under a constraint to prevent rigid body motion, this constraint would affect the real compressive residual stress, because each constraint side will not allow the gap between the upper sheet and lower sheet of the laminated composites. In the riveting simulation, the energy analysis showed that kinetic energy is negligible compared with internal energy.

B. Optimal Maximum Force

Four maximum forces (25,000, 30,000, 35,000, and 40,000 N) defined by the sine wave force history of the riveting force were

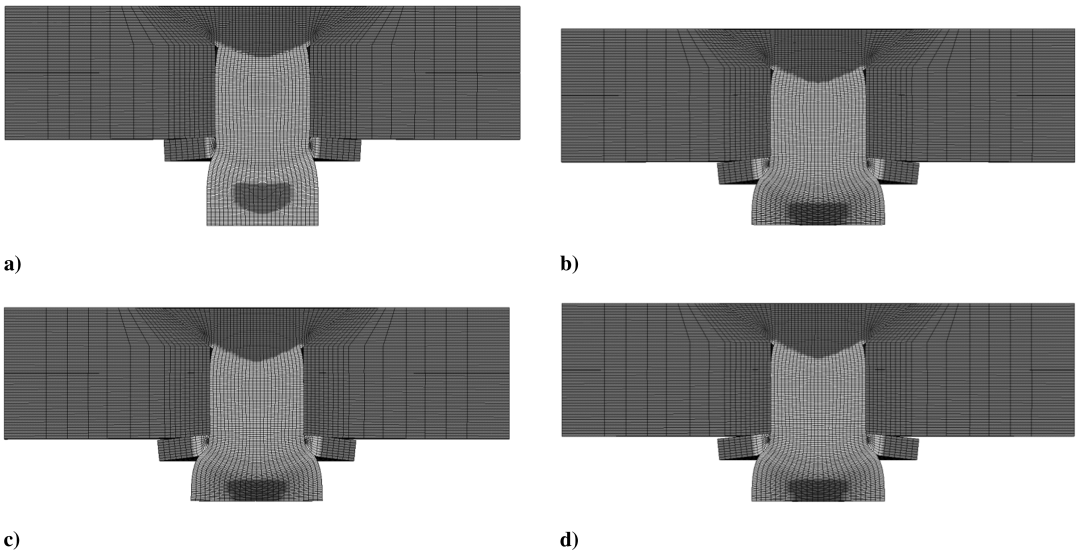

Fig. 8 Plastic strain of rivet from riveting process: a) 0.25 ms, b) 0.50 ms, c) 0.75 ms, and d) 1.00 ms.

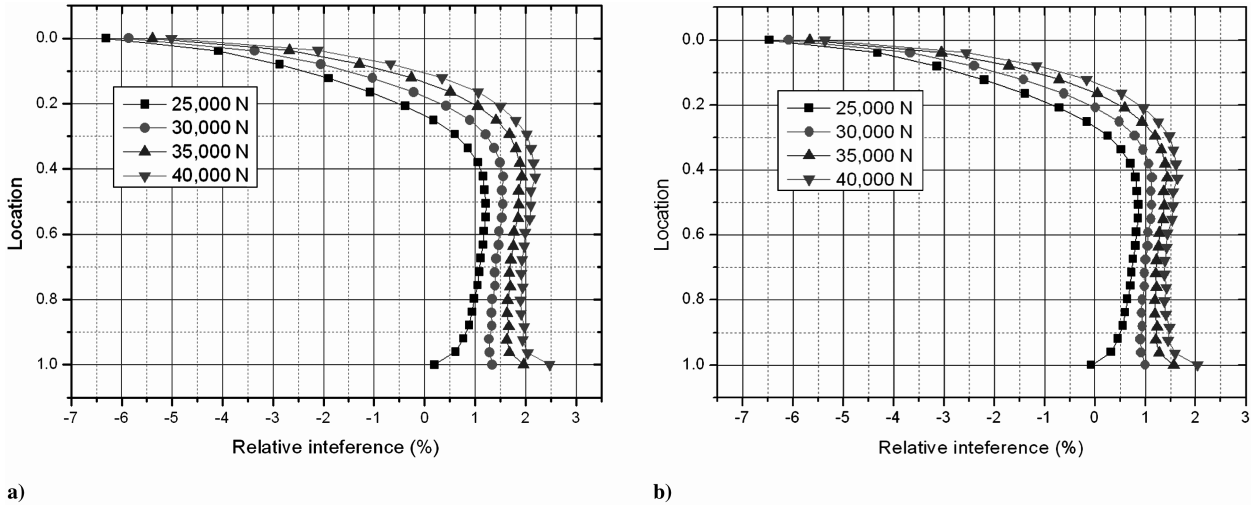

Fig. 9 Relative interference with force (25,000, 30,000, 35,000, and 40,000 N): a) end of loading step and b) end of unloading step.

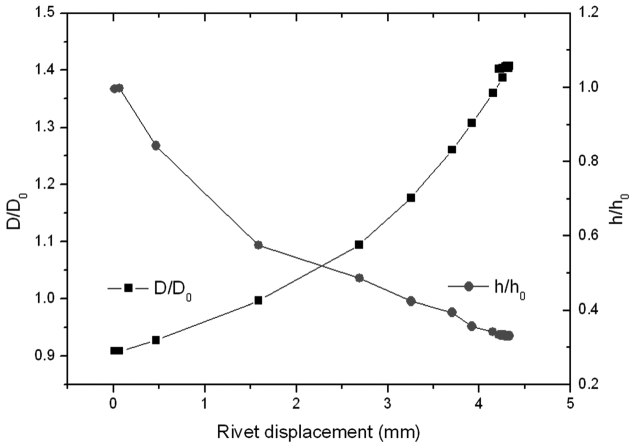

Fig. 10 Rivet-tail deformation.

investigated to find the optimal maximum force that will not only enhance the fatigue life but also protect against any failure of the riveted joint in the laminated composites. Figure 9 shows the rivet displacement for the four maximum forces. As the maximum force is increased, the rivet displacement is also increased. In this study, the 2% relative interference criterion of a laminated composite for extending fatigue life was used [4,11]. Relative interference in the loading step was larger than that in the unloading step at all locations along the rivet shaft, and the largest relative interference was shown at the end of the loading step. In the case of the maximum force of 40,000 N, the relative interference was over 2% at the end of the loading step in Fig. 9a. This maximum force would not be feasible for riveting in laminated composites. For 25,000, 30,000, and 35,000 N, the relative interference was under 2% at the end of the loading step. The optimal maximum force was found from the trial and error method at the end of the loading step based on the 2% relative interference criterion. So, the optimal maximum force of 35,800 N was obtained.

Figure 10 shows the parameters associated with rivet-tail deformation. The rivet is observed to buckle under loading. As the applied force increases, rivet displacement is generated, and then the diameter ratio (D/D_0) of the shaft increases and the height ratio (h/h_0) decreases. The design rule of thumb dictates that D/D_0 should fall within the range of 1.3–1.8 in metallic structures [1,2]. Although a D/D_0 of 1.4 was, in our case, for the maximum force of 35,800 N after the riveting process, another criterion should be prepared, because a special washer is used in composite structures, unlike in metallic structures.

C. Compressive Residual Stress

An optimal maximum force of 35,800 N of the sine wave force history and 1 ms of riveting time for the EMR were applied in the investigation of the compressive residual stress. Radial and tangential stress distributions between the bottom layer of the upper sheet and the top layer of the lower sheet on the faying surface were compared at the end of the loading step and at the end of the unloading step. In Fig. 11, the radial and tangential stress distributions along the lateral direction from location 0.3 (point B of Fig. 6) are shown. The radial stress and tangential stress change from compression stress to tension stress along the lateral direction, and they become zero stress away from the rivet shaft, as shown in Fig. 11. The maximum compressive radial stress and the maximum compressive tangential stress of the bottom layer of the upper sheet are larger than those of the top layer of the lower sheet. The maximum compressive radial stress of the bottom layer of the upper sheet at the end of the loading step was 35% larger than that at the end of the unloading step, and maximum compressive tangential stress of the bottom layer of the upper sheet at the end of the loading step was 22% larger than that at the end of unloading step. The bottom layer of the upper sheet and the top layer of the lower sheet on the faying surface are oriented at a 45 deg fiber angle, so radial and tangential residual stress distribution may not be balanced. In Fig. 12, the through-the-thickness variation of the radial directional shear stress and tangential directional shear stress are shown according to the fiber angle of the laminated composite, but in the case of a homogenized model, the layer effect is not shown. Maximum radial directional shear stress is shown at locations 1.0 (point A) and 0.0 (point C) in Fig. 12a, and maximum tangential directional shear stress is shown at location 1.0 and location $0.0 \sim 0.2$ in Fig. 12b. The laminas carrying maximum shear stress may cause failure in laminated composites, and they will have to be carefully examined during the riveting process. The refined riveting simulation provided a more accurate description of the stress distribution beneath the rivet head that occurred during high-speed riveting than the experiment did. Therefore, riveting simulation is advantageous in the design of a riveted joint in laminated composites.

D. Effect of Force History

The sine wave riveting force history was used in the riveting simulation using the EMR riveter. When a conventional riveter, such as a hydraulic riveter, is used, the linear force history of a pneumatic riveter is often selected for riveting simulations [2]. So, the sine wave force history and the linear force history were compared to find their differences. The relative interference obtained using the sine wave force history and that obtained using the linear force history were similar near location 0.3 and location 1.0 on the faying surface, but the internal energy and stress distributions were a little different

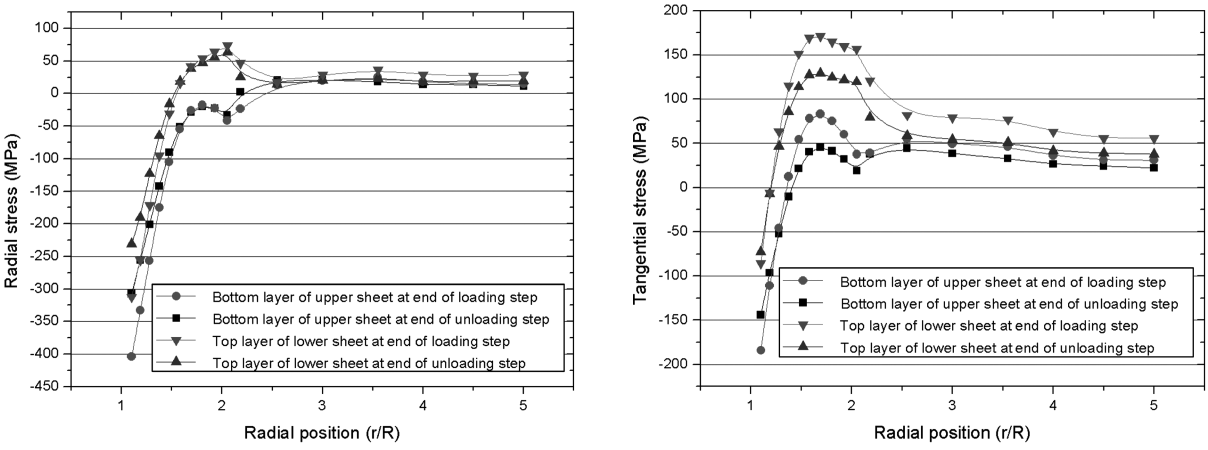

a) b)

Fig. 11 Stress distribution on faying surface (lateral direction): a) radial stress and b) tangential stress.

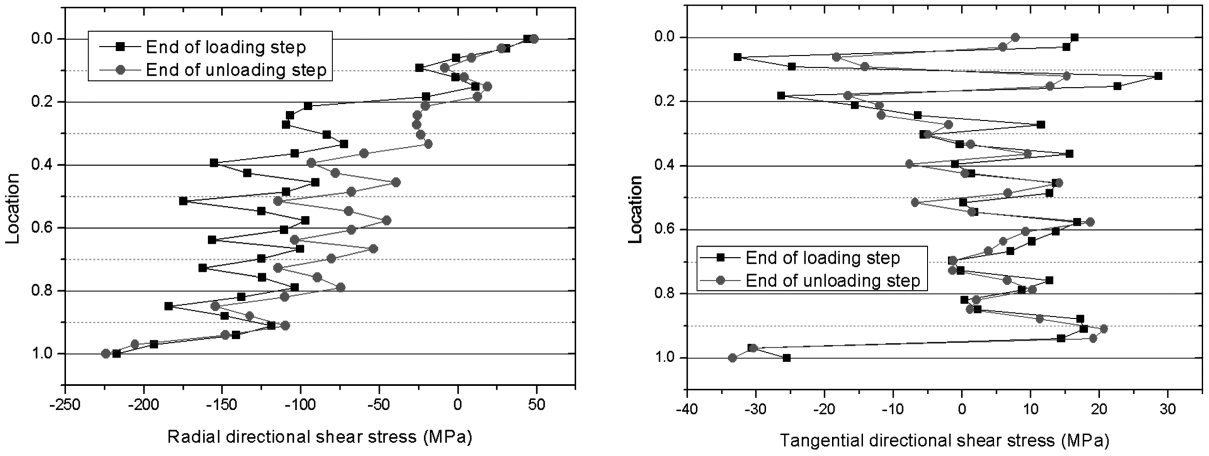

a) b)

Fig. 12 Shear stress distribution of through-the-thickness direction: a) radial direction and b) tangential direction.

between these two force histories. When an EMR riveter is used for riveting, the linear force history can be used to estimate the proper stress distributions, and the riveting simulation can be avoided.

E. Effect of Mesolevel Model

The mesolevel model is considered by the fiber angle of each layer in laminated composites, while the homogenized model is considered to be transversely isotropic in all layers of laminated composites. The refined modeling with the mesolevel model of the laminated composites and the simplified modeling with the homogenized model of the laminated composites were compared to examine the layer effects on riveting in laminated composites. The relative interference between the mesolevel model and the homogenized model was compared at the end of the loading step because of the large relative interference that occurred at the end of the loading step, which greatly increased the possibility of failure. The relative interference of the homogenized model was larger than that of the mesolevel model at the end of the loading step, and the homogenized model gave overestimated results. As the clamping force by riveting was increased, a gap was generated and slip gradually occurred on the faying surface because of the abrupt changes in the radial directional displacement of the aperture wall between the upper and lower sheets on the faying surface. The radial directional shear stress in the through-the-thickness direction also suddenly changed on the faying surface, as shown in Fig. 13a, because the homogenized model may be considered stiffer than the mesolevel model. Stress distributions of the mesolevel model showed the layer effects properly, but those of the homogenized model did not show layer effects, as shown in Fig. 13.

F. Effect of Washer

A washer dimension is characterized by the ratio of the outer diameter divided by the inner diameter, and this ratio affects the quality of a riveted joint in laminated composites [4]. The riveting model of Fig. 2 was used as the base model under the maximum force of 35,800 N of the sine wave force history and the riveting time of 1.0 ms. Four washer dimensions (1.5, 2.2. 2.5, and 3.0) were examined to obtain the proper riveting process with relative uniform interference. The washer dimension of 2.2 corresponded to the washer dimension of the base model. Washer dimensions of 2.5 and 3.0 have similar uniform relative interference as the washer dimension of 2.2: the base model. However, in the cases of washer dimensions 2.5 and 3.0, the gap between the washer and the lower sheet of the laminated composites was larger than the gap of the base model because of the relatively larger washer outer diameter. The model with the washer dimension of 1.5 had nonuniform interference, and its relative interference was greater than the 2% relative interference criterion. Therefore, the washer dimension of 2.2 was determined to be the proper washer model for the EMR riveting.

Three washer thicknesses (0.8, 1.0, and 1.2 mm) were examined to obtain the proper riveted joint in laminated composites. The washer thickness of 1.0 mm corresponded to the washer thickness of the base model. The interference among the three types was nearly the same, but the relative interference increased as the washer thickness

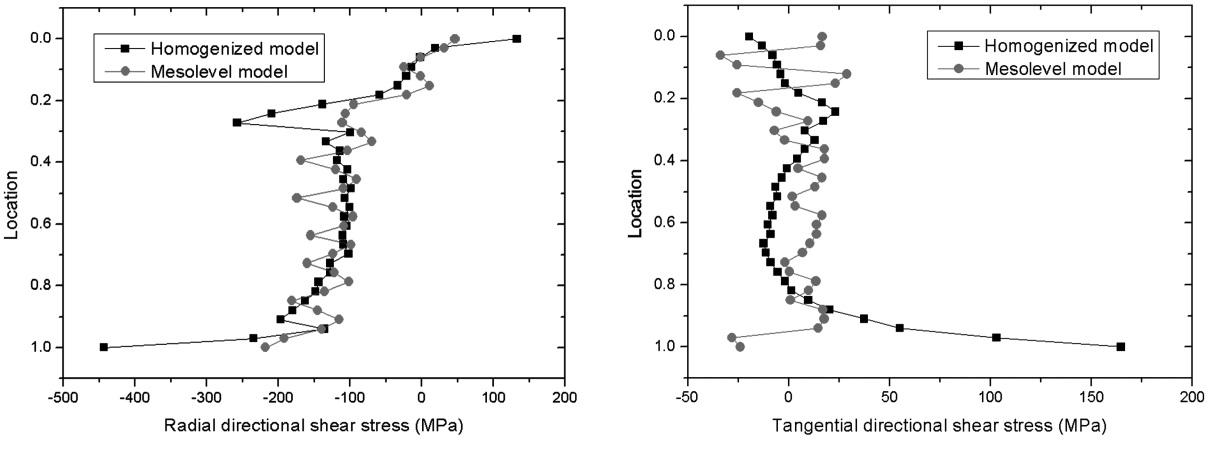

a) b)

Fig. 13 Shear stress distribution on faying surface by homogenized model at end of loading step (through-the-thickness direction): a) radial direction and b) tangential direction.

Table 3 Elapsed time of parallel computing by IBM machine at KISTI

CPUs	Elapsed time
8	4 h 24 min
16	2 h 53 min
32	1 h 41 min

increased. Rivet displacement decreased as the washer thickness increased. However, in the case of the washer thickness of 0.8 mm, the gap between the lower sheet of the laminated composites and the washer was large, so the model for this case may not be considered as the proper model of a riveted joint in laminated composites. Therefore, the washer thickness of 1.0 or 1.2 mm was determined to be the proper washer model for the EMR riveting.

G. Effect of Computer Resources

Parallel computing is effective in dealing with detailed modeling and mesh sensitivity. However, computing costs may be expensive, so various numerical techniques, such as mass scaling, time scaling, and half- or quarter-mesh modeling are used to save calculation time [1,16]. Refined modeling of riveting in laminated composites, which is required to reflect the physical characteristics of complicated contacts in riveting simulations properly, is analyzed by parallel computing technologies. A parallel version of MPP in LS-DYNA was used to analyze the refined modeling in two parallel computing systems: one is the Pegasus system (Xeon 2.2, 2.4, 2.8, and 3.0 GHz clock speed, 520 CPUs) in our laboratory, in which LS-DYNA/V970 was installed, and the other is the IBM system (POWER5+ 2.3 GHz clock speed, 640 CPUs) at the supercomputing center of KISTI, in which LS-DYNA/V971 was installed. The IBM machine at KISTI is the newer of the two systems.

As shown in Table 3, the calculation time of the riveting simulation by parallel computing decreases as the number of CPUs increases. However, the proper number of CPUs has to be considered with respect to computation cost and time for riveting modeling analysis, because the scalability of parallel computing decreases as the number of CPUs increases. The riveting simulation carried out with 16 CPUs in the IBM machine at KISTI (2 h 53 min) is about four times faster than that carried out with 16 CPUs of 2.2 GHz in the Pegasus system (10 h 28 min). So, the parallel computing system is important for decreasing calculation time, although the computation cost becomes more expensive as the number of CPUs increases and/or the system is renewed.

The riveting time of the refined EMR 3-D modeling was 1 ms, but a longer riveting time is required for a typical riveter. Numerical simulation time is usually accumulated as simulation time increases, and so, in the case of a typical riveter, more computing power or other numerical techniques may be needed.

VI. Conclusions

1) Numerical simulation of riveting in composite structures using the EMR riveter was conducted by full 3-D refined modeling for the sine wave of riveting force history. Refined modeling was considered by mesolevel composite modeling with fiber angles in each layer and a washer inner fillet geometry. Relative uniform interference through the rivet shaft by the EMR riveter was validated with the experimental literature.

2) The optimal maximum riveting force for the model was obtained by the trial and error method from a few simulations using the relative interference criterion for fatigue life extension at the end of the loading step. Relative interference was examined by the riveting simulation for two load steps: the loading step and the unloading step. The largest relative interference and compressive residual stress distribution existed at the end of the loading step during the riveting process, which may have affected failure initiation. Relative uniform interference was shown, and maximum relative interference was located at the bottom of the lower sheet under the optimal maximum riveting force.

3) One of the important control methods of riveting in composite structures is the use of a special washer. The effects of washer dimension and washer thickness were analyzed by parametric studies using detailed riveting modeling, and design changes were rapidly reflected by the parallel computing environment. These parametric studies with refined riveting modeling reflecting the washer effect will be effectively applied for the design change of a riveted joint in composite structures. However, the computing cost and elapsed time of a riveting simulation in parametric studies will have to be controlled effectively.

Acknowledgments

This research was supported by the National Space Laboratory program through the National Research Foundation of Korea funded by the Ministry of Education, Science and Technology (2009-0092052), the Defense Acquisition Program Administration, and the Agency for Defense Development under contract UD100048JD.

References

[1] Rans, C. D., Alderliesten, R. C., and Straznicky, P. V., "Effects of Rivet Installation on Residual Stress and Secondary Bending in a Riveted Lap Joint," 48th AIAA Structures, Structural Dynamics, and Materials Conference, Honolulu, HI, AIAA Paper 2007-2307, April 2007.

[2] Rans, C. D., Alderliesten, R. C., and Straznicky, P. V., "Riveting Process Induced Residual Stresses Around Solid Rivets in Mechanical Joints," *Journal of Aircraft*, Vol. 44, No. 1, 2007, pp. 323–329. doi:10.2514/1.23684

[3] Deng, J. H., Yu, H. P., and Li, C. F., "Numerical and Experimental Investigation of Electromagnetic Riveting," *Materials Science and Engineering A*, Vol. 499, Nos. 1–2, 2009, pp. 242–247. doi:10.1016/j.msea.2008.05.049

[4] Cao, Z., and Cardew-Hall, M., "Interference-Fit Riveting Technique in Fiber Composite Laminates," *Aerospace Science and Technology*, Vol. 10, No. 4, 2006, pp. 327–330. doi:10.1016/j.ast.2005.11.003

[5] Holleman, E., and Muller, R. P. G., "Parametric Study of Rivet Squeezing in GLARE 3 3/2-0/2. GLARE 3 3/2-0.3 and 2024-T3," Delft Univ. of Technology, Faculty of Structures and Materials Lab. Rept. BE 2040, Delft, The Netherlands, June 1995.

[6] Kang, J., and Johnson, W. S., "Analysis of the Cold Working Process of Holes Containing Preexisting Cracks," *Journal of Aircraft*, Vol. 42, No. 5, 2005, pp. 1281–1287. doi:10.2514/1.11842

[7] Sendeckyj, G. P., and Richardson, M. D., "Fatigue Behavior of a Graphite-Epoxy Laminate Forced Through an Interference Fit Pin," *Proceedings of the 2nd Air Force Conference on Fibrous Composites in Flight Vehicle Design*, U.S. Air Force Flight Dynamics Lab. TR 74-103, Sept. 1974, pp. 469–520.

[8] Chakherloua, T. N., and Vogwellb, J., "The Effect of Cold Expansion on Improving the Fatigue Life of Fastener Holes," *Engineering Failure Analysis*, Vol. 10, No. 1, 2003, pp. 13–24. doi:10.1016/S1350-6307(02)00028-6

[9] Ofsthun, M., "When Fatigue Quality Enhancers do Not Enhance Fatigue Quality," *International Journal of Fatigue*, Vol. 25, Nos. 9–11, 2003, pp. 1223–1228. doi:10.1016/S0142-1123(03)00122-1

[10] Brown, A. M., and Straznicky, P. V., "Simulating Fretting Contact in Single Lap Splices," *International Journal of Fatigue*, Vol. 31, No. 2, 2009, pp. 375–384. doi:10.1016/j.ijfatigue.2008.07.012

[11] Cole, R. T., Baten, E. J., and Potter, J., "Fasteners for Composite Structures," *Composites*, Vol. 13, No. 3, 1982, pp. 233–240. doi:10.1016/0010-4361(82)90005-2

[12] Liu, P., and Zhang, K., "An Experimental Study on Fatigue Life of Interference-Fit Joint," *Acta Aeronautica et Astronautica Sinica*, Vol. 12, No. 12, 1991, pp. 545–549.

[13] Tong, Y., and Qu, L., "Recent Patents in Riveting and Applications," *Recent Patents on Engineering*, Vol. 3, No. 3, 2009, pp. 220–227. doi:10.2174/187221209789117799

[14] Perley, W., and Zieve, P., "Lightweight HH503 Handheld Riveter," *SAE Aerofast Conference*, Chester, England, U.K., Soc. of Automotive Engineers, Warrendale, PA, 2002. doi:10.4271/2002-01-2631

[15] Cao, Z., and Qin, Q., "A Study on Driving Interference-fit Fastener Using Stress Wave," *Materials Science Forum*, Vols. 532–533, 2006,

pp. 1–4.
doi:10.4028/www.scientific.net/MSF.532-533.1

[16] Li, G., Shi, G., and Bellinger, N., "Study of the Residual Strain in Lap Joints," *Journal of Aircraft*, Vol. 43, No. 4, 2006, pp. 1145–1151.
doi:10.2514/1.18125

[17] Iyer, K., Rubin, C. A., and Hahn, G. T., "Influence of Interference and Clamping on Fretting Fatigue in Single Rivet-Row Lap Joints," *Journal of Tribology*, Vol. 123, No. 4, Oct. 2001, pp. 686–698.

[18] Atre, A., "A Finite Element and Experimental Investigation on the Fatigue of Riveted Lap Joints in Aircraft Applications," Ph.D. Dissertation, School of Mechanical Engineering, Georgia Inst. of Technology, Atlanta, GA, 2006.

[19] Langrand, B., Deletombe, E., Markiewicz, E., and Drazétic, P., "Riveted Joint Modeling for Numerical Analysis of Airframe Crashworthiness," *Finite Elements in Analysis and Design*, Vol. 38, No. 1, 2001, pp. 21–44.
doi:10.1016/S0168-874X(01)00050-6

[20] Makino, M., "The Performance of 10-Million Element Car Model by MPP Version of LS-DYNA on Fugitsu PRIMEPOWER," *10th International LS-DYNA Users Conference*, LSTC, Dearborn, MI, June 2008, pp. 5-7–5-10.

[21] Kim, S. J., Paik, S. H., Ji, K. H., and Yoon, T. H., "3-D Riveting Process Simulation of Laminated Composites," *Key Engineering Materials*, Vols. 334–335, 2007, pp. 405–408.
doi:10.4028/www.scientific.net/KEM.334-335.405

[22] Yoon, T. H., and Kim, S. J., "Refined Simulation of Riveting on Composite Materials Using Parallel Computing," *ICCES Special Symposium on Meshless and Other Novel Computational Methods (ICCES-MM)*, Busan, ROK, edited by J. K. Palik and S. N. Alturi, Aug. 2010, pp. 62–64.

[23] Mamalis, A. G., and Manolakos, D. E., "Electromagnetic Forming and Powder Processing: Trends and Developments," *Applied Mechanics Reviews*, Vol. 57, No. 4, July 2004, pp. 229–324.
doi:10.1115/1.1760766

[24] Shang, J., L'Eplattenier, P., Wilkerson, L., and Hatkevich, S., "Numerical Simulation and Experimental Study of Electromagnetic Forming," *11th International LS-DYNA Users Conference*, LSTC, Dearborn, MI, June 2010, pp. 10-27–10-35.

[25] Repetto, E. A., Radovitzky, R., Ortiz, M., Lundquist, R. C., and Sandstrom, D. R., "A Finite Element Study of Electromagnetic Riveting," *Journal of Manufacturing Science and Engineering*, Vol. 121, No. 1, 1999, pp. 61–68.
doi:10.1115/1.2830576

[26] LS-DYNA Software Package, Ver. 971, Livermore Software Technology Corp., Livermore, England, U.K., 2007.

[27] Srinivasan, S., Wang, H., Taber, G. A., and Daehn, G. S., "Dimensional Control and Formability in Impact Forming," *4th International Conference on High Speed Forming*, Columbus, Ohio, Technische Univ.Dortmund, Inst. Umformtechnik, Dortmund, Germany, 2010, pp. 239–249.

[28] Ekh, J., and Schon, J., "Force Transfer in Multirow, Single Shear, Composite-to-Aluminium Lap Joints," *Composites Science and Technology*, Vol. 66, Nos. 7–8, 2006, pp. 875–885.
doi:10.1016/j.compscitech.2005.08.015

[29] Linde, P., and De Boerm, H., "Modelling of Inter-Rivet Buckling of Hybrid Composites," *Composite Structures*, Vol. 73, No. 2, 2006, pp. 221–228.
doi:10.1016/j.compstruct.2005.11.062